Diagnostic value of ^{68}Ga-DOTA-TATE PET/CT imaging for tumor-induced osteomalacia

Yu Zhang[1,2], Xiaolin Zhang[3], Wei Zhang[1,2], Zhanwen Huang[1,2], Yue Chen[1,2]

[1]Department of Nuclear Medicine, Affiliated Hospital of Southwest Medical University, Luzhou, China; [2]Nuclear Medicine and Molecular Imaging Key Laboratory of Sichuan Province, Luzhou, China; [3]Drug Clinical Trial Institution, Affiliated Hospital of Southwest Medical University, Luzhou, China

Contributions: (I) Conception and design: Y Zhang, Y Chen; (II) Administrative support: X Zhang; (III) Provision of study materials or patients: Y Zhang, X Zhang, W Zhang, Z Huang; (IV) Collection and assembly of data: All authors; (V) Data analysis and interpretation: Y Zhang, W Zhang, Z Huang, Y Chen; (VI) Manuscript writing: All authors; (VII) Final approval of manuscript: All authors.

Correspondence to: Yue Chen. Department of Nuclear Medicine, Affiliated Hospital of Southwest Medical University; Nuclear Medicine and Molecular Imaging Key Laboratory of Sichuan Province. No. 25, Taiping St., Luzhou 646000, China. Email: yuzhang309@163.com.

Background: Tumor-induced osteomalacia (TIO) is often misdiagnosed as hypophosphatemia that is not valued. The aim of this study was to analyze the diagnostic value of ^{68}Ga-DOTA-TATE PET/CT imaging for TIO.

Methods: Clinical data was retrospectively collected for 56 patients with suspected TIO at the Affiliated Hospital of Southwest Medical University between January 2016 and December 2019, where patients were examined by ^{68}Ga-DOTA-TATE PET/CT and ^{99m}Tc-HYNIC-TOC SPECT. Based on the results of the patient's surgery, the diagnostic efficacy of the two imaging techniques on TIO were analyzed.

Results: Of the 56 patients, 41 were diagnosed with TIO, with phosphorus levels ranging from 0.25 to 0.75 mmol/L. The remaining 15 patients were non-TIO. Results of ^{99m}Tc-HYNIC-TOC SPECT showed 33 cases were positive, with a diagnostic sensitivity, specificity, and accuracy of 58.54%, 86.67%, and 66.07%, respectively. Results of ^{68}Ga-DOTA-TATE PET/CT imaging showed 46 cases were positive, with a diagnostic sensitivity, specificity, and accuracy of 95.13%, 60.00%, 71.43%, respectively. The average tumor size with ^{68}Ga-DOTA-TATE PET/CT imaging was 2.58±1.71 cm. The lesions of 41 patients involved bone and soft tissue, while 18 patients showed osteolytic bone destruction. Distribution was mainly under the skin, followed by intermuscular space, and cortex of bone. Compared with muscle density, the lesions showed uniformly or slightly lower density nodules. Using ^{99m}Tc-HYNIC-TOC SPECT, the planar imaging of 30 patients showed that radioactive uptake increased at the early stage, and it can be accurately positioned on the SPECT imaging.

Conclusions: The ^{68}Ga-DOTA-TATE PET/CT imaging demonstrated high accuracy in the diagnosis of TIO and detected small lesions, which could provide more comprehensive information for clinicians, and provide a reference value for the treatment and prognosis of patients.

Keywords: ^{68}Ga-DOTA-TATE PET/CT imaging; tumor-induced osteomalacia (TIO); diagnostic value

Introduction

In clinical practice, hypophosphatemia is diagnosed as either primary or secondary hypophosphatemia [X-linked hypophosphatemia (XLH) or tumor-induced osteomalacia (TIO), respectively]. TIO was first reported in 1947 (1). Tumor is the causative factor of osteomalacia (2), with the condition alleviated once the tumor is removed (3). TIO is a chronic disorder rarely seen in clinical practice, and as of 2016, a total of 350 cases have been reported (4). However, due to its relatively insidious onset, its slow progression, and poor clinical awareness, TIO is often misdiagnosed as hypophosphatemia, and not treated appropriately. Surgical removal of patients' tumors is often performed to achieve the pathogenic purpose, therefore it is important to correctly locate the lesions involved in the diagnosis. Yet tumors causing TIO are small and widely distributed in the body, they cannot be accurately located with conventional imaging. The use of auxin receptor imaging is an effective way in the diagnosis and treatment of TIO (5,6). Therefore, this study aimed to analyze the diagnostic value of ^{68}Ga-DOTA-TATE PET/CT in TIO. We present the following article in accordance with the STARD reporting checklist (available at http://dx.doi.org/10.21037/apm-20-1466).

Methods

General information

Clinical data of suspected TIO patients at the Affiliated Hospital of Southwest Medical University between January 2016 to December 2019 were collected. A total of 56 patients were identified comprising 33 males and 23 females aged from 20 to 60 years, with an average age of 45.30±10.36 years. The disease course of patients ranged from 1 to 20 years, with an average course of 6.46±2.13 years. The inclusion criteria were as follows: (I) patients with complete clinical data and laboratory data; (II) patients with suspected clinical TIO, excluding hypophosphatemic osteomalacia caused by genetic factors, primary hyperparathyroidism, renal tubular poisoning and other factors; (III) patients who voluntarily joined the study and signed an informed consent. The exclusion criteria were as follows: (I) patients with active infections and immunodeficiency diseases; (II) patients with other liver diseases or systemic diseases involving the liver; (III) patients with contraindications for related examinations. All procedures performed in this study involving human participants were in accordance with the Declaration of Helsinki (as revised in 2013). This study was approved by the ethics committee of the Affiliated Hospital of Southwest Medical University (No.20083). The informed consent was taken from all the patients.

^{68}Ga-DOTA-TATE PET/CT examination

(I) Preparation of ^{68}Ga-DOTA-TATE: 5 mL of 0.1 mmol/L hydrochloric acid was used to rinse the Ge/^{68}Ga generator to make ^{68}Ga stock solution. The pH value was adjusted to 3.5–4.0 with sodium acetate (1.25 mol/L). Twenty µg of DOTA-TATE (ABX, Germany) was added to the solution and mixed, which was then heated at 100 ℃ for 10 min and cooled at room temperature. After cooling, the solution was filtered using a sterile filter to obtain ^{68}Ga-DOTA-TATE injection. The radiochemical purity was analyzed using the thin layer chromatography method to be >95%.

(II) ^{68}Ga-DOTA-TATE PET/CT examination: The equipment (Biograph 64 Truepoint TrueV PET/CT, Germany) was first examined. Patients removed all metal items from their person. Patients were given intravenous ^{68}Ga-DOTA-TATE (2–5 mCi), and PET/CT examination was performed 30 min later, with scanning range from cranial crest to foot sole. CT was used for attenuation correction and reconstructed with OSEM. Siemens MMWP workstation was used as post-processing program.

^{99m}Tc-HYNIC-TOC SPECT imaging examination

One mL of fresh ^{99m}TcO-4 eluent (radioactivity concentration of 999 MBq/mL) was added to the HYNIC‑TOC ligand solution, followed by 25 µL of stannous chloride solution. After mixing, the solution was left at room temperature for 1 hour. Labeling rate was determined to be >97%. Patients were intravenously injected with 350–400 MBq ^{99m}Tc-HYNIC-TOC for 1 to 4 hours, then whole-body images of patients were collected. The imaging device was a dual-probe SPECT instrument: Millennium VG & Hawkeye system (GE company, USA); E.CAM180 (Siemens, Germany); IRIX (Philips, Netherlands), using a low-energy and high-resolution parallel hole collimator with an energy peak of 140 keV and a window width of 20%. For the suspected TIO lesions in the whole-body planar imaging, SPECT imaging was conducted in the corresponding part, and the matrix was 128×128, 40 s/frame. Ordered subset expectation

Table 1 Comparison of the diagnostic effectiveness of different examinations for tumor-induced osteomalacia (TIO)

Examination technology	Cases	Sensitivity	Specificity	Accuracy
^{99m}Tc-HYNIC-TOC SPECT	56	58.54% (24/41)	86.67% (13/15)	66.07% (37/56)
^{68}Ga-DOTA-TATE PET/CT	56	95.13% (39/41)	60.00% (9/15)	71.43% (40/56)

maximization (OSEM) was used to reconstruct the images.

Image analysis

The images were independently analyzed by two experienced nuclear medicine doctors. If opinions differed, the doctors discussed it until a consensus was reached. In ^{68}Ga-DOTA-TATE PET/CT, a positive determination of TIO was required to meet the following conditions (7): (I) abnormal local radiation uptake concentration; (II) one-machine CT examination with or without obvious abnormal density change; (III) nonspecific uptake lesions caused by fracture, necrosis of the femoral head, arthritis or other disorders had been excluded.

Observation indicators

The images obtained from the patients were analyzed. Based on the follow-up surgical pathology results, the diagnostic efficacy of different imaging examinations on TIO was calculated.

Statistical methods

The data in this study were statistically analyzed using SPSS 28.0 software (IBM, USA). Measurement data were described as the mean ± standard deviation. The count data was expressed as passing rate or composition ratio and analyzed using the χ^2 test. Results with P<0.05 were considered statistically different.

Results

Comparison of the diagnostic efficiency of different examinations for TIO

Of the 56 patients included in the study, 41 were diagnosed with TIO, with phosphorus levels ranging from 0.25–0.75 mmol/L (normal reference range: 0.81–1.45 mmol/L), and clinical manifestations of fracture, inconvenience, fatigue, and bone pain. The remaining 15

patients were diagnosed as non-TIO.

Using ^{99m}Tc-HYNIC-TOC SPECT, 33 patients were positive: 24 true positives and 9 false positives. The remaining 23 patients were negative: 13 true negatives and 10 false negatives. The results showed that the diagnostic sensitivity, specificity, and accuracy of the image examination were 58.54%, 86.67%, 66.07%, respectively.

With ^{68}Ga-DOTA-TATE PET/CT, 46 patients were positive: 39 true positives and 7 false positives. Ten patients were negative: 9 true negatives and 1 false negative. The sensitivity, specificity and accuracy of TIO diagnosis were 95.13%, 60.00%, and 71.43%, respectively, suggesting that the sensitivity and accuracy of ^{68}Ga-DOTA-TATE PET/CT examination for TIO diagnoses were higher than that of ^{99m}Tc-HYNIC-TOC SPECT examination, while the specificity was lower than ^{99m}Tc-HYNIC-TOC SPECT imaging examination (*Table 1*).

Image analysis results

With ^{68}Ga-DOTA-TATE PET/CT imaging, the size of the tumor lesions of patients was 0.57–7.56 cm, with the average tumor size of 2.58±1.71 cm. The lesions of 41 patients involved bone and soft tissue, of which 29 cases involved bone, 12 cases were in the lower extremity, 7 cases were in the trunk, 9 cases were in the upper or lower jaw, and 1 case in the upper limb. Among them, 1 patient's imaging showed that the lesion involved bone and soft tissue at the same time; 18 patients showed osteolytic bone destruction; 7 cases showed sclerosing bone changes with focal bone density increase; 4 cases showed expansive bone destruction occurring in the rib lesions and the surrounding soft tissues were involved; discontinuous destruction of the bone cortex was seen in 3 cases; no obvious bone changes were seen in 2 cases. There were 11 cases located in soft tissues, and the lesions were mainly distributed under the skin, followed by muscle space, paracortical bone and other tissues, which showed uniformly or slightly lower density nodules, compared with muscle density. Clear boundaries were seen in 7 of the 11 cases. Blurred boundaries with surrounding muscles were observed in 4 cases. Most cases
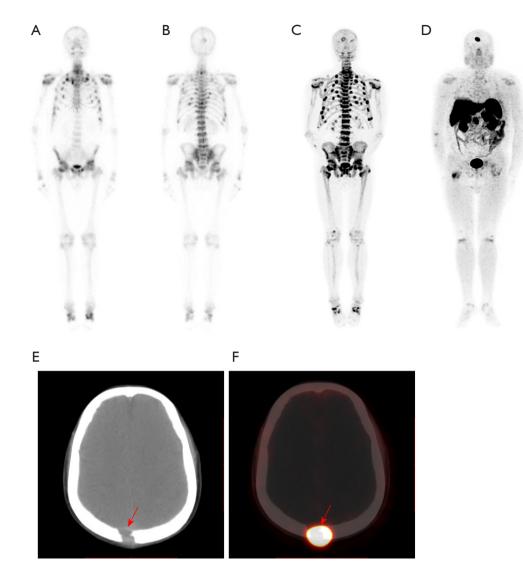
Figure 1 Imaging analysis of a typical case of tumor-induced osteomalacia (TIO). (A,B,C) Bone imaging of ^{99m}Tc-MDP. (D,E,F) Bone imaging of ^{18}F-NaF. ^{68}Ga-DATA-TATE PET/CT tomographic fusion imaging image (E: low-dose CT), (F: fusion image): as indicated by the arrow, the right parietal bone is osteolytic bone destruction with increased imaging agent intake, SUVmax is about 14.8, this is the tumor lesion of TIO.

had uniform density. In ^{99m}Tc-HYNIC-TOC SPECT, 30 patients with planar imaging showed that the radioactive uptake increased early, and it could be accurately positioned on the SPECT imaging.

Analysis of a typical case

One male patient aged 48 years, reported experiencing whole body pain for 5 years, particularly in his bilateral hip joints, and could no longer walk. The results of ^{99m}Tc-MDP bone imaging and 18F-NaF bone imaging suggested that the patient had osteolytic bone destruction on the right parietal bone and multiple systemic fractures, and was undergoing symptomatic treatment (*Figure 1A,B,C*). The subsequent ^{68}Ga-DOTA-TATE imaging showed osteolytic bone destruction on the right parietal bone combined with increased somatostatin receptor (SSTR) expression, suggesting tumor-associated low-phosphorus chondrosis lesions (TIO). Surgical resection was recommended. Postoperative medical examination indicated it to be

phosphaturic mesenchymal tumor. After the operation, the patient's symptoms gradually alleviated (*Figure 1D,E,F*).

Discussion

A clear diagnosis of TIO is difficult in clinical practice. TIO is caused by hypophosphatemia and bone mineralization disorders associated with tumors, but rarely shows obvious clinical symptoms. Even if the patient has reduced blood phosphorus, there is no specificity for clinically distinguishing the patient's lesion (8,9). The majority of TIO patients suffer from severe systemic symptoms, which significantly reduce the quality of life. The main therapy of TIO treatment is completely surgical resection. Once the clinical symptoms of patients are relieved and the blood phosphorus is restored after resection, the final diagnosis of TIO is established (10).

With traditional imaging showing limitations in clinical diagnosis, better diagnostic methods are urgently needed. Molecular imaging technology is an advanced diagnostic method with molecular imaging agents being extensively researched. There is evidence that various mesenchymal tissues are derived from the expression of SSTR in tumors, especially the SSTR2 receptor. Therefore, in the examination of TIO pathogenic tumors, the imaging examination of SSTRs has become the main clinical examination method (11). The ^{68}Ga-labeled somatostatin receptor octreotide (^{68}Ga-DOTA-TOC, ^{68}Ga-DOTA-NOC, ^{68}Ga-DOTA-TATE) is a kind of positron display agent. It is reported that the use of single-electron imaging agents has a good diagnostic effect on TIO, with high sensitivity and specificity (12). In the study of Ferrero *et al.* (13), it was found that the sensitivity, specificity, and accuracy in locating the tumors causing TIO were all above 85.00%, but in actual clinical work, some patients' lesions were still negative. The ^{68}Ga-labeled somatostatin receptor octreotide has the advantage of simple synthesis process, high labeling in the body, and with the similar clearance time in the human body to the peptide molecule (14). In recent years, the expression of SSTR has played an important role in tumor examination. Studies have found that by comparing the ^{111}In-octreotide with ^{68}Ga-labeled somatostatin receptor octreotide, the latter had stronger binding effect to SSTR2 and better tumor uptake. Lin *et al.* found that ^{68}Ga-DOTA-TATE PET/CT had high value in the examination of neuroendocrine tumors, and is better than ^{99m}Tc-HYNIC-TOC and 111In-octreotide SPECT imaging examination for the detection of small

lesions or complex structural lesions (15). A study by Yücel *et al.* found that the PET imaging showed better image resolution than the SPECT image when comparing the ^{99m}Tc-HYNIC-TOC SPECT with ^{68}Ga-DOTA-TATE PET/CT (16). Tumor volume in TIO is generally small, resulting in a missed diagnosis of small lesions or lesions with low uptake by SPECT. The PET/CT can obtain a whole-body tomographic image in one examination and can detect lesions that are missed in planar imaging due to overlapping of organs. Furthermore, the PET/CT shows a strong binding with SSTR2, which also improves the detection rate of lesions.

In this study, based on the images obtained by PET examination, we saw increased expression as well as the location of SSTRs, which were combined with the CT images to help determine the TIO pathogenic focus (17). The sensitivity, specificity and accuracy of ^{68}Ga-DOTA-TATE PET/CT imaging for TIO detection were 95.13%, 60.00% and 71.43%, respectively, indicating that the ^{68}Ga-DOTA-TATE PET/CT examination has higher sensitivity and accuracy for TIO diagnosis than ^{99m}Tc-HYNIC-TOC SPECT imaging examination. However, specificity was lower than with ^{99m}Tc-HYNIC-TOC SPECT examination, which was consistent with the published literature discussed above. In 35 cases of TIO, the tumors were single, and the lesions mostly involved the limbs. According to the origin of the tissue, the lesions were mostly located in bone tissue, which was also consistent with the results of previous studies (18). We discovered that lesions in patient bone tissue could manifest as osteolytic bone destruction, and there were a few patients with sclerotic changes. There was some misdiagnosis, which may have been caused by increased ossification in the patient's body. We also found that 12 patients (41.37%) had lesions in the lower extremities which rarely involved the surrounding soft tissues. There was no specificity of distribution of lesions in soft tissue, because the lesions could both exist under the skin and in the muscle space. SSTR can also express on the surface of inflammatory cells, for which ^{68}Ga-DOTA-TATE PET/CT has a high sensitivity (19,20). In clinical practice, there may also be false positive lesions caused by non-specific inflammation, post-fracture inflammatory repair, and other inflammation. Therefore, it is necessary to combine local CT images during examination, and further examination is needed for those who have no obvious abnormal changes in bone.

In summary, ^{68}Ga-DOTA-TATE PET/CT imaging detects small lesions and provides a higher accuracy in the

diagnosis of TIO. This can provide more comprehensive information for clinicians, and provide a reference value for the treatment and prognosis of patients.

Footnote

References

1. McCANCE RA. Osteomalacia with Looser's nodes (Milkman's syndrome) due to a raised resistance to vitamin D acquired about the age of 15 years. Q J Med 1947;16:33-46.

2. Prader A, Illig R, Uehlinger E, et al. Rickets following bone tumor. Helv Paediatr Acta 1959;14:554-65.

3. Zhong M, Geng H, Zhu W, et al. Comments on "Altered gait mechanics are associated with severity of chondropathy after hip arthroscopy for femoroacetabular impingement syndrome". Gait Posture 2020. [Epub ahead of print].

4. Unterrainer M, Maihoefer C, Cyran CC, et al. 68Ga-DOTATATE PET/CT reveals epstein-barr virus-associated nasopharyngeal carcinoma in a case of suspected sphenoid wing meningioma. Clin Nucl Med 2018;43:287-8.

5. Babazadeh NT, Schlund DJ, Cornelius T, et al. Should 68Ga-DOTATATE PET/CT be performed routinely in patients with neuroendocrine tumors before surgical resection? World J Surg 2020;44:604-11.

6. Brown-Taylor L, Wilson J, McNally M, et al. Altered gait mechanics are associated with severity of chondropathy after hip arthroscopy for femoroacetabular impingement syndrome. Gait Posture 2020;77:175-81.

7. Raj N, Reidy-Lagunes D. The role of 68Ga-DOTATATE positron emission tomography/computed tomography in well-differentiated neuroendocrine tumors: A case-based approach illustrates potential benefits and challenges. Pancreas 2018;47:1-5.

8. Filippi L, Bagni O, Schillaci O. Re: Hepatocellular carcinoma mimicking neuroendocrine tumor metastasis on 68Ga-DOTATATE PET/CT. Clin Nucl Med 2020;45:258-9.

9. Gomes Gobbi R, Pastore E Silva AL, Kawamura Demange M, et al. Clinical results of pulsed signal therapy on patellofemoral syndrome with patellar chondropathy. Bioelectromagnetics 2019;40:83-90.

10. Bolfa P, Dennis M, Grevemeyer B, et al. Histopathological characterization and proposed prognostic predictors in equine arytenoid chondrosis/chondropathy. J Comp Pathol 2019;166:105.

11. Zollner B, Ganswindt U, Maihöfer C, et al. Recurrence pattern analysis after [68Ga]-DOTATATE-PET/CT -planned radiotherapy of high-grade meningiomas. Radiat Oncol 2018;13:110.

12. Aso K, Shahtaheri SM, Hill R, et al. Associations of symptomatic knee osteoarthritis with histopathologic features in subchondral bone. Arthritis Rheumatol 2019;71:916-24.

13. Ferrero G, Sconfienza LM, Fiz F, et al. Effect of intra-articular injection of intermediate-weight hyaluronic acid

on hip and knee cartilage: in-vivo evaluation using T2 mapping. Eur Radiol 2018;28:2345-55.

14. Cherk MH, Kong G, Hicks RJ, et al. Changes in biodistribution on 68Ga-DOTA-Octreotate PET/CT after long acting somatostatin analogue therapy in neuroendocrine tumour patients may result in pseudoprogression. Cancer Imaging 2018;18:3.

15. Lin X, Shao W, Yu F, et al. Individual and combined toxicity of T-2 toxin and deoxynivalenol on human C-28/I2 and rat primary chondrocytes. J Appl Toxicol 2019;39:343-53.

16. Yücel D, Aydoğdu S, Cehreli S, et al. Increased oxidative stress in dilated cardiomyopathic heart failure. Clin Chem 1998;44:148-54.

17. Kim S, Dillon WP, Hope TA, et al. Ectopic Thyroid-Stimulating Hormone-Secreting Pituitary adenoma of the nasopharynx diagnosed by gallium 68 DOTATATE positron emission tomography/computed tomography. World Neurosurg 2019;125:400-4.

18. Gasongo G, Greenbaum LA, Niel O, et al. Effect of nonsteroidal anti-inflammatory drugs in children with Bartter syndrome. Pediatr Nephrol 2019;34:679-84.

19. Gabriel S, Garrigue P, Dahan L, et al. Prospective evaluation of 68Ga-DOTATATE PET/CT in limited disease neuroendocrine tumours and/or elevated serum neuroendocrine biomarkers. Clin Endocrinol (Oxf) 2018;89:155-63.

20. Sundin A. Novel Functional Imaging of Neuroendocrine Tumors. Endocrinol Metab Clin North Am 2018;47:505-23.

(English Language Editor: J. Brown)